WIMS-AECL MULTICELL CALCULATIONS FOR BURNUP HETEROGENEITY

I.S. Hong and B. Rouben
Reactor Core Physics Branch
Atomic Energy of Canada Limited
2251 Speakman Drive
Mississauga, ON
Canada L5K 1B2
hongis@aecl.ca, roubenb@aecl.ca

Abstract

The burnup heterogeneity effect in the ACR™-1000 was investigated using the WIMS-AECL multicell (MC) calculation capability, which allows the calculation of lattice properties taking into account the effects of neighbour cells. The MC calculations were performed with WIMS-AECL version 3.1.1, based on a 3×3 group of cells with the ACR-1000 fuel at various burnup values. The MC results for the central cell were then compared to those obtained with the standard single-cell (SC) calculation. While the MC model does not reproduce exactly the SC values, the reactivity differences are bounded by the values; -4.82 mk and +1.45 mk, which are small relative to the absolute SC reactivity values; +143 mk for fresh fuel and -38 mk for exit-burnup fuel, respectively. Considering that these differences tend to cancel out over the bundle residence time in the core, it is concluded that there is no strong need to replace the SC calculation with the MC calculation for routine time-average or core-tracking simulations.

1. INTRODUCTION

The multicell (MC) calculation capability has been implemented in WIMS-AECL [1] to allow calculations of lattice properties taking into account the effects of neighbour cells. This allows a more realistic calculation of cell properties than is possible with single-cell (SC) calculations. This is expected to be especially important in the case of high heterogeneity between neighbouring cells. Three specific configurations with high heterogeneity in the ACR-1000 have been identified as particularly appropriate for investigation using the MC capability: checkerboard coolant voiding [2], partially defuelled channels (during refuelling operations), and the core-reflector interface.

However, it is important to verify MC results for other configurations as well. Here, the MC calculations on 3×3 and 2×2 models were employed in order to investigate the effects of burnup heterogeneity on lattice-cell reactivity and homogenized lattice cross sections. The effects were investigated for conditions at different positions in the core, as well as for different burnups.

All calculations were performed with the latest WIMS-AECL version 3.1.1, and the MC results were compared to those obtained with the standard SC calculation.

Advanced CANDU Reactor™ is a trademark of Atomic Energy of Canada Limited

2. APPROACH

An intermediate design for the ACR-1000 fuel, design "Option 5", was used. The reactor has a 24-cm lattice pitch, and the fuel has 2.0 % uranium enrichment in all rings except the centre pin, which consists of natural uranium with burnable poison. The refuelling scheme for this fuel is the 8 bundle-shift scheme.

Figure 1 shows the 3×3 MC model used in this work, as well as the standard SC model. The cell of interest is the central cell (C) in the 3×3 group. Various configurations were modelled, with the fuel in the cell of interest at zero-burnup, mid-burnup [5,848 MWd/Mg(U)], and exit-burnup [11,678 MWd/Mg(U)]. Depending on the configuration, the neighbour cells had fuel at mid-burnup, low-burnup [1,172 MWd/Mg(U)] and/or high-burnup [11,123 MWd/Mg(U)]. The latter two values of burnup correspond to the average burnup of fuel in the first (inlet-end) and the last (outlet-end) bundle positions in fuel channels.

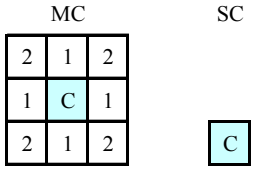

Figure 1 Model Configurations for Multicell and Single-Cell Calculations

One set of configurations modelled here is for a cell surrounded by mid-burnup cells. These arise in bundle positions 5-8 in a channel, as a new bundle enters the core in one of these positions and proceeds through mid and high burnup, with, on average, mid-burnup fuel surrounding it at any time.

The other set of configurations modelled here corresponds to cells at the inlet or outlet ends of fuel channels. For a bundle at the first 4 bundle positions in a channel, i.e., at the inlet positions 1-4, we modelled a fresh cell surrounded by four high-burnup fuel bundles as nearest neighbours radially (cell type 1 in Figure 1) and four low-burnup fuel bundles diagonally (cell type 2 in Figure 1). For a bundle position at the outlet positions 9-12, we modelled an exit-burnup cell surrounded by four low-burnup fuel bundles as nearest neighbours radially and four high-burnup fuel bundles diagonally. These configurations were modelled to simulate the extreme cases at the ends of fuel channels. However, it was recognized that a 3×3 model for these configurations results in duplicate cells at the outer cell boundary. A corrective methodology is presented in Section 3.2, to take these effects into account.

The major configurations of interest are summarized in Table 1. Fresh, mid-burnup and exit-burnup were used for the central cell of interest (cell type C in Figure 1) in the MC model. Mid-burnup, high-burnup and low-burnup values were used variously for the neighbour cells (cell types 1 and 2).

Figure 2 illustrates the calculation procedure for the comparison of each MC and SC calculation set. SC depletion calculations were performed from zero to exit-burnup, both to generate SC reference lattice properties and to generate fuel compositions, which were

used as input to MC calculations. Then the MC results for the central cell were compared with SC results. Both k_∞ and 2-group macroscopic cross sections were compared.

Table 1
Cell Configurations for Burnup Conditions

Single-Cell Burnup	Multicell Burnup	Hypothetic Cell Position
cell C: **Fresh**	cell C : **Fresh**, cell 1 : Mid, cell 2 : Mid	Middle of Channel (5-8)
	cell C : **Fresh**, cell 1 : High, cell 2 : Low	Inlet End (1-4)
cell C: **Mid**	cell C : **Mid**, cell 1 : Mid, cell 2 : Mid	Middle of Channel (5-8)
cell C: **Exit**	cell C : **Exit**, cell 1 : Low, cell 2 : High	Outlet End (9-12)
	cell C : **Exit**, cell 1 : Mid, cell 2 : Mid	Middle of Channel (5-8)

* Burnups [MWd/Mg(U)] :
Fresh – 0.0, Mid – 5848.2, Exit – 11677.8, Low – 1172.0, High – 11123.0.

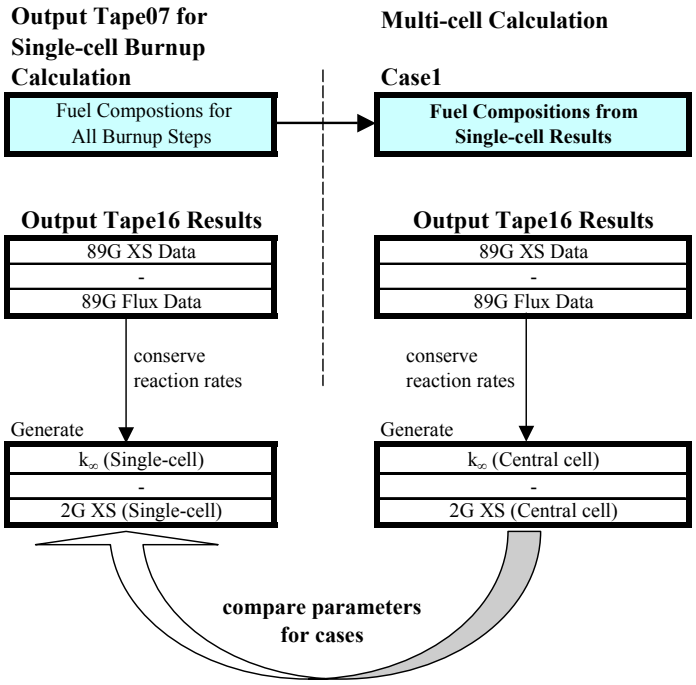

Figure 2 Calculation Flowchart

3. METHODOLOGIES

3.1 Post Processing of Output Data

It should be noted that, in MC calculations of the present WIMS-AECL, the k_∞ is calculated for the entire multicell where intra-cell leakage is taken into account. Therefore, the k_∞ that is printed out in MC calculations cannot be directly compared with that of SC calculations. Neither can the 2-group cell cross sections which are printed out.

Thus, in order to make meaningful comparisons of the reactivity and 2-group cell properties from MC and SC calculations, flux and cross sections were calculated using

the general condensation equations [3], making use of cell-averaged data saved on the WIMS-AECL 89-group tape16 output file.

On the other hand, a "virtual" infinite-multiplication-factor was defined for multi-group M, as

$$virtual\ k_{\infty,M} = \frac{\sum_{g=1}^{M}\chi_g \sum_{g'=1}^{M}\nu\Sigma_{fg'}\phi_{g'}}{\sum_{g=1}^{M}\Sigma_{ag}\phi_g} = \frac{\sum_{g=1}^{M}\nu\Sigma_{fg}\phi_g}{\sum_{g=1}^{M}\Sigma_{ag}\phi_g},\ \sum_{g=1}^{M}\chi_g = 1.0\,, \qquad (1)$$

which is analogous to the conventional definition of infinite multiplication factor. Where g denotes condensed energy-group index, χ_g and ϕ_g stand for the g-group fission spectrum and neutron flux, respectively.

This Eq. (1) satisfies Eq. (2), where scattering terms do not contribute to net production or loss:

$$virtual\ k_{\infty,M} = \frac{production\ \ rate}{loss\ rate\ \ without\ \ leakage}. \qquad (2)$$

Throughout this paper, $virtual\ k_{\infty,M}$ is simply denoted as k_∞.

It is to be noted that the equations for the 2-group condensation are designed to conserve the 89-group reaction rates, and consequently the 2-group k_∞ is equal to the 89-group k_∞ also.

3.2 Model Correction for Channel End Positions

The MC configurations, with fresh or exit-burnup cells of interest, and neighbouring cells at combinations of low and high burnup, were modelled to investigate the radial heterogeneity effect at the inlet or outlet ends of a channel.

Figure 3 shows the two target MC configurations at the inlet and outlet ends, respectively. The first configuration arises at the inlet end, where a fresh cell is surrounded by four high-burnup fuel bundles as nearest neighbours radially and four low-burnup fuel bundles diagonally. The second configuration arises at the outlet end, where the exit-burnup central cell is surrounded by four low-burnup fuel bundles as nearest neighbours radially and four high-burnup fuel bundles diagonally. F and E represent fresh and exit-burnup fuels, and H and L denote high- and low-burnup fuels, respectively.

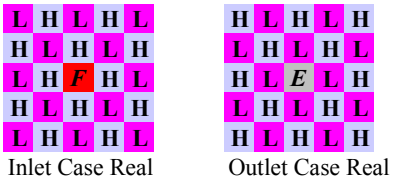

Figure 3 Target Multicell Configurations at Inlet and Outlet

The configurations in Figure 3 could be obtained using a model with larger number of cells, but a 3×3 MC model was used instead, on account of computational restrictions of the WIMS-AECL version, both in computer memory and computing time.

Note that if the periodic or reflective boundary condition of the WIMS-AECL is applied to the 3×3 configuration, the resultant configurations become those in Figure 4. That is, four repeated cells and two repeated cells are located in diagonal and radial directions, respectively, instead of the checkerboard-pattern cells in Figure 3.

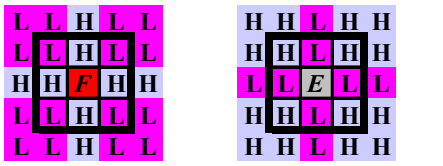

Inlet Case1 : (3x3) Outlet Case1: (3x3)

Figure 4 WIMS-AECL 3×3 Multicell Configurations at Inlet and Outlet

Some correction is therefore necessary to estimate the effects from the duplicate cells at the 3×3 lattice boundary. Additional lattice models were used to estimate these corrections: Figure 5 shows two sets of 2×2 and 3×3 MC configurations for inlet and outlet ends, respectively, to estimate the effects of the duplicate cells. The periodic boundary condition was applied to these models. It must be noted that the 2×2 lattice model with checkerboard-pattern can exactly replace the realistic model for this case, which consists of only two types of cells. By comparing the first and second figures in Figure 5, one can estimate the effect of duplicate cells, i.e., the reactivity difference between the 2×2 and the incomplete 3×3 lattice models can be used as a correction factor.

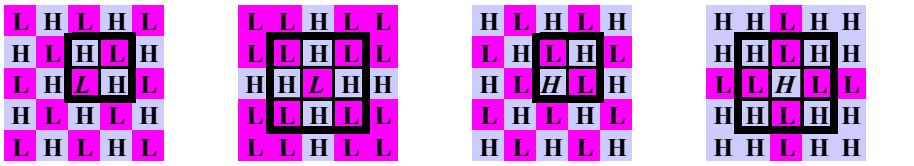

Inlet Case2 : (2x2) Inlet Case3 : (3x3) Outlet Case2: (2x2) Outlet Case3: (3x3)

Figure 5 Additional Multicell Configurations for k_∞ Correction at Channel Inlet and Outlet

In the present study, the correction was estimated for the reactivity ρ only. That is, the ρ values for the target inlet and outlet configurations of "Case Real" in Figure 3 were approximated by correcting the ρ of the incomplete 3×3 "Case 1" configurations in Figure 4 using the equation below:

$$\rho(\text{Case Real}) \approx \rho(\text{Case 1 : 3x3}) + \Delta\rho\,, \tag{3}$$

where the correction was calculated as

$$\Delta\rho = \{\rho(\text{Case 2 : 2x2}) - \rho(\text{Case 3 : 3x3})\} \times \frac{\rho(\text{Case 1 : 3x3})}{\rho(\text{Case 3 : 3x3})}\,. \tag{4}$$

It should be noted that in Eq. (4) the burnup effect of the central cell was taken into account by normalizing by the reactivity ratio of "Case 1" to that of "Case3".

The above equations can be simplified into the equation below.

$$\rho(\text{Case Real}) \approx \rho(\text{Case 2 : 2x2}) \times \frac{\rho(\text{Case 1 : 3x3})}{\rho(\text{Case 3 : 3x3})}. \quad (5)$$

4. NUMERICAL RESULTS

4.1 Cells Surrounded by Mid-Burnup Fuel Cells: Middle Positions in a Channel

These configurations were devised to reflect possible situations in the middle bundle positions (5-8) in a fuel channel.

Three MC calculations were performed for zero-burnup, mid-burnup and exit-burnup central cells surrounded by mid-burnup cells. Results were compared with those from SC calculations for each burnup state.

Table 2 summarizes the k_∞ values for the three burnup values investigated. For the fresh cell, the MC k_∞ exhibits a lower reactivity than the SC k_∞ by 4.82 mk. In contrast, for the exit-burnup cell, the MC k_∞ exhibits a higher reactivity than the SC k_∞ by 1.45 mk. For the mid-burnup cell, the MC and SC k_∞ are essentially equal (as they should be).

Table 2
k_∞ Comparison of Single-Cell and Multicell with Mid-Burnup Neighbour Cells

Cell Burnup	Single-Cell		Multicell (b)	Reactivity Diff (mk) (c)
	WIMS-AECL Output	Calculated from Tape16 89G Cell Averaged Data (a)	Calculated from Tape16 89G Cell Averaged Data	
Fresh	1.166870	1.166847	1.160326	-4.82
Mid	1.053340	1.053313	1.053318	0.00
Exit	0.963260	0.963239	0.964589	1.45

(a)

$$k_{\infty,MG} = \frac{\sum_{g=1}^{M} \nu\Sigma_{fg}\phi_g}{\sum_{g=1}^{M} \Sigma_{ag}\phi_g}, \; M : number \quad of \quad Energy \quad groups \; .$$

(b) Neighbor cell configuration : all mid-burnup fuels.

(c) { $1/k_\infty$ (single-cell calculated) - $1/k_\infty$(multicell calculated) } x 1000.

Thus, the difference in reactivity between the MC and SC models starts out as negative for fresh fuel, vanishes for mid-burnup fuel, and thereafter turns positive. While the MC model does not reproduce exactly the SC values, the differences in k_∞ (- 4.82 mk for fresh fuel and +1.45 mk for exit-burnup fuel) are considered small relative to the absolute SC reactivity values (+143 mk for fresh fuel and -38 mk for exit-burnup fuel) – see Figure 6 in section 4.2. Since the fuel-reactivity difference tends to approximately cancel out over the entire burnup history of the fuel in these configurations, the SC treatment of

lattice properties for the burnup-induced heterogeneity is judged sufficiently accurate for routine calculations, e.g., time-average or core-tracking simulations.

The basic-lattice cross sections, as calculated with both the SC and MC models, are shown in Table 3. Individual cross-section differences are seen to be fractions of a percent in most cases; only the yield and scattering cross sections for fresh and exit-burnup fuel exhibit differences greater than 1%.

Table 3
2G Cell Properties for Single-Cell vs. Multicell with Mid-burnup Neighbour Cells

Cell Burnup	Cell Parameters		Single-Cell	Multicell (a)	Rel. Diff [%] (b)
Fresh	Absorption Cross Section [cm^{-1}]	Fast	2.65272E-03	2.66279E-03	0.38
		Thermal	7.51102E-03	7.55723E-03	0.62
	Yield Cross Section [cm^{-1}]	Fast	1.43124E-03	1.45538E-03	1.69
		Thermal	1.01984E-02	1.02559E-02	0.56
	Transport Cross Section [cm^{-1}]	Fast	2.39695E-01	2.39320E-01	-0.16
		Thermal	3.82534E-01	3.82472E-01	-0.02
	Scattering Cross Section [cm^{-1}]	Down	8.88583E-03	8.69277E-03	-2.17
		Up	1.46081E-04	1.50743E-04	3.19
	Relative Flux (c) [$n/(cm^2s)$]	Fast	8.79686E+01	9.11698E+01	3.64
		Thermal	1.02069E+02	1.00200E+02	-1.83
	k_∞		1.166847	1.160326	- 4.82 mk
Mid	Absorption Cross Section [cm^{-1}]	Fast	2.77248E-03	2.77299E-03	0.02
		Thermal	7.67958E-03	7.67817E-03	-0.02
	Yield Cross Section [cm^{-1}]	Fast	1.28125E-03	1.28170E-03	0.04
		Thermal	9.55220E-03	9.55068E-03	-0.02
	Transport Cross Section [cm^{-1}]	Fast	2.39899E-01	2.39893E-01	0.00
		Thermal	3.82434E-01	3.82441E-01	0.00
	Scattering Cross Section [cm^{-1}]	Down	8.76981E-03	8.76921E-03	-0.01
		Up	1.48128E-04	1.48097E-04	-0.02
	Relative Flux [$n/(cm^2s)$]	Fast	8.79122E+01	8.79133E+01	0.00
		Thermal	9.84774E+01	9.84893E+01	0.01
	k_∞		1.053313	1.053318	0.00 mk
Exit	Absorption Cross Section [cm^{-1}]	Fast	2.88313E-03	2.87697E-03	-0.21
		Thermal	7.45340E-03	7.44161E-03	-0.16
	Yield Cross Section [cm^{-1}]	Fast	1.15003E-03	1.12107E-03	-2.52
		Thermal	8.60607E-03	8.59300E-03	-0.15
	Transport Cross Section [cm^{-1}]	Fast	2.40097E-01	2.40526E-01	0.18
		Thermal	3.83118E-01	3.83008E-01	-0.03
	Scattering Cross Section [cm^{-1}]	Down	8.66522E-03	8.88372E-03	2.52
		Up	1.43148E-04	1.43214E-04	0.05
	Relative Flux [$n/(cm^2s)$]	Fast	8.78449E+01	8.63842E+01	-1.66
		Thermal	1.00187E+02	1.00983E+02	0.79
	k_∞		0.963239	0.964589	1.45 mk

(a) Neighbor cell configuration : all mid-burnup fuels.

(b) Cross Sections : (MC - SC)/SC x 100, Reactivity Difference (mk) : $\{1/k_\infty(SC) - 1/k_\infty(MC)\}$x1000.

(c) Normalized to the absorption rate of 1.0.

* Note that the boundary between fast group and thermal goup is 0.625 eV.

4.2 Cells Surrounded by Checkerboard-Pattern Low- and High-Burnup Fuels: End Positions in a Channel

These configurations, with fresh or exit-burnup cells of interest, and neighbouring cells at combinations of low and high burnups, were modelled to investigate the heterogeneity effect at the inlet end positions (1-4) or outlet end positions (9-12) of a channel - see Section 3.2 for detailed methodology.

Table 4 summarizes the k_∞ values for the corrected cases as well the uncorrected cases, at the inlet and outlet ends of a channel.

For the fresh cell surrounded by high- and low-burnup cells (Inlet Case1), both the uncorrected and corrected MC k_∞ values exhibit a lower reactivity than the SC k_∞, by 2.79 mk and 3.93 mk respectively. Note that both of these values are smaller than the underestimate for the fresh cell surrounded by mid-burnup cells (4.82 mk – see Table 2).

For the exit-burnup cell surrounded by low- and high-burnup cells (Outlet Case1), the uncorrected MC k_∞ exhibits a lower reactivity than the SC k_∞ by 0.08 mk, but the corrected MC k_∞ is higher than the SC k_∞ by 1.16 mk. Again, this difference is smaller than that for the exit-burnup cell surrounded by mid-burnup cells (1.45 mk – see Table 2).

Considering that these cases represent extreme configurations at the channel ends, and that the differences between MC and SC results are smaller than those for the configurations in the middle positions in a channel, the difference between the MC and SC k_∞ values is estimated to be bounded by the values -4.82 mk and +1.45 mk for a bundle in any position in a channel, throughout its residence time in the core.

Table 4
k_∞ Comparison of Single-Cell and Multicell with Multi-burnup Cells

Case	k_∞			Reactivity diff (mk) (b) uncorrected	Reactivity diff (mk) corrected
	Single-cell	Multicell uncorrected	Multicell corrected (a)		
Inlet Case 1	1.166847	1.163055	1.161521	-2.79	-3.93
Outlet Case 1	0.963239	0.963164	0.964312	-0.08	1.16

(a) Corrected from Case 1 to Case Real using equation (5).

(b) { $1/k_\infty$ (single-cell calculated) - $1/k_\infty$(multicell calculated)} x 1000.

Figure 6 compares the SC and MC k_∞ values for the bundle positions in a channel as well as for burnup. Comparing the k_∞ differences between MC and SC for the inlet and outlet end positions, the difference in reactivity between the MC and SC models starts out as negative at the inlet end, and turns positive at the outlet end. This observation is also consistent with the observation for cells at middle positions in a channel. It is also observed that the differences in reactivity between MC and SC models are quite acceptable for routine calculations even for the extreme configurations at inlet and outlet ends of channels.

The basic-lattice cross sections are shown in Table 5 for the inlet Case 1 and outlet Case 1. Individual cross-section differences are seen to have smaller values than in Table 3.

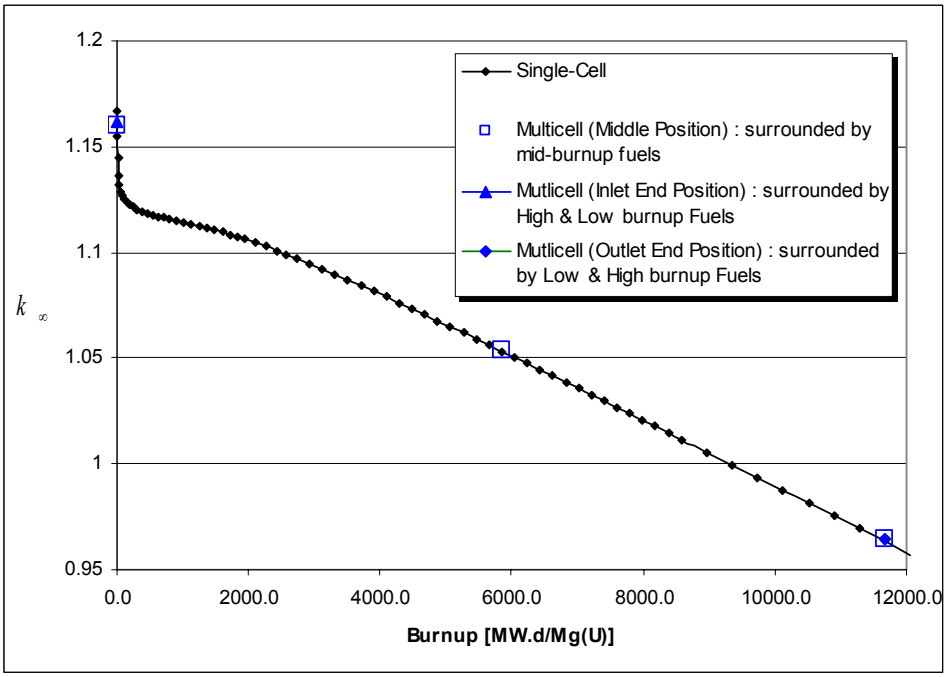

Figure 6 k_∞ Values for Cell Burnup and Positions

Table 5
2G Cell Properties for Single-Cell vs. Multicell at Channel Ends

Case	Cell Cross Sections		Single-Cell	Multicell	Rel. Diff (%)
Inlet Case1	Absorption Cross Section [cm^{-1}]	Fast	2.65272E-03	2.66833E-03	0.59
		Thermal	7.51102E-03	7.53610E-03	0.33
	Yield Cross Section [cm^{-1}]	Fast	1.43124E-03	1.46669E-03	2.48
		Thermal	1.01984E-02	1.02295E-02	0.30
	Transport Cross Section [cm^{-1}]	Fast	2.39695E-01	2.39188E-01	-0.21
		Thermal	3.82534E-01	3.82582E-01	0.01
	Scattering Cross Section [cm^{-1}]	Down	8.88583E-03	8.68879E-03	-2.22
		Up	1.46081E-04	1.48208E-04	1.46
	Relative Flux [$n/(cm^2s)$]	Fast	8.79686E+01	9.01691E+01	2.50
		Thermal	1.02069E+02	1.00768E+02	-1.27
	k_∞		1.166847	1.163055	-2.79 mk
Outlet Case1	Absorption Cross Section [cm^{-1}]	Fast	2.88313E-03	2.87354E-03	-0.33
		Thermal	7.45340E-03	7.45205E-03	-0.02
	Yield Cross Section [cm^{-1}]	Fast	1.15003E-03	1.11974E-03	-2.63
		Thermal	8.60607E-03	8.60570E-03	0.00
	Transport Cross Section [cm^{-1}]	Fast	2.40097E-01	2.40497E-01	0.17
		Thermal	3.83118E-01	3.82989E-01	-0.03
	Scattering Cross Section [cm^{-1}]	Down	8.66522E-03	8.80761E-03	1.64
		Up	1.43148E-04	1.43865E-04	0.50
	Relative Flux [$n/(cm^2s)$]	Fast	8.78449E+01	8.71646E+01	-0.77
		Thermal	1.00187E+02	1.00580E+02	0.39
	k_∞		0.963239	0.963164	-0.08 mk

5. CONCLUSIONS

Multicell (MC) models based on a 3×3 group of cells have been applied using WIMS-AECL to various configurations with burnup heterogeneity, which arise in a reactor during normal conditions.

In order to compare the properties of the central cell of interest in the MC model to those of the single cell (SC) model, two categories of calculations were performed for conditions at both the middle and the end positions in a channel. The MC and SC models showed some difference in both k_∞ and cross sections, however, the difference in k_∞ values was bounded by the values -4.82 mk and +1.45 mk for a bundle in any position in a channel, throughout its residence time in the core. In the context of core-tracking calculations, these differences are considered to be acceptable, especially since they tend to cancel out over the residence time of a bundle in the core. Therefore, on the basis of these results for the burnup-induced heterogeneity, it is concluded that there is no strong need to replace single-cell calculations with multicell calculations for routine calculations, e.g., time-average or core-tracking simulations.

6. REFERENCES

[1] J.D. Irish and S.R. Douglas, "Validation of WIMS-IST", Proceedings of the 23rd Annual Conference of the Canadian Nuclear Society, Toronto, Ontario, Canada, June 2-5, 2002.

[2] W. Shen, "Recent Progress in the Development of Cross-section Models in the Reactor Fuelling Simulation Program (RFSP)", *Mathematics and Computation, Supercomputing, Reactor Physics and Nuclear and Biological Applications* Palais des Papes, Avignon, France, September 12-15, 2005, on CD-ROM, American Nuclear Society, LaGrange Park, IL (2005).

[3] James J. Duderstadt and Louis J. Hamilton, " Nuclear Reactor Analysis", John Wiley & Sons, Inc., 1976.